Turkish Journal of Electrical Engineering & Computer Sciences

http://journals.tubitak.gov.tr/elektrik/

Research Article

Turk J Elec Eng & Comp Sci
(2020) 28: 1164 – 1178

doi:10.3906/elk-1907-161

Fast adaptive reclosing in double-circuit transmission lines for improving power system stability based on harmonic analysis scheme

Mohsen JANNATI[1,*], **Ali Akbar AKBARI**[2]
[1]Department of Engineering, University of Shahreza, Shahreza, Iran
[2]Khomeini Shahr Branch, Islamic Azad University, Isfahan, Iran

Received: 21.07.2019 • **Accepted/Published Online:** 01.10.2029 • **Final Version:** 28.03.2020

Abstract: An appropriate method is proposed for identifying permanent faults from transient faults in double-circuit transmission lines. This method could be used in adaptive single phase auto-reclosures in order to diagnose between permanent and transient faults, determine extinguishing time of the secondary arc, and calculate issuing time of reclosing commands during the occurrence of transient single phase to ground faults. The proposed method is based on harmonic analysis of the adjacent healthy circuit and could be an effective solution for blocking permanent disconnection of the power flow, improving stability, and maintaining the power network synchronism. In this paper, transient and permanent faults are simulated on a typical power system, and then current harmonics of the healthy circuit terminal are extracted and finally the proposed index for identifying the fault type is applied. In the case of transient faults, this method determines the minimum time needed for a fast successful adaptive reclosing in the network and thus prevents instability and nonsynchronism in both sides of the transmission line. Results of the various simulations run in EMTP-RV verifies accurate performance of the proposed approach.

Key words: Transient and permanent faults, double-circuit transmission lines, single phase auto-reclosure, EMTP-RV

1. Introduction

Single line to ground (SLG) faults in transmission lines (TLs) are classified into two types: permanent and transient. About 80% of TL SLG faults are single phase to ground, in which 80% of the cases have transient nature [1]. Therefore, it is not necessary to disconnect all three phases when a short circuit SLG fault occurs. In such a situation, single-phase reclosures are employed to block permanent power disconnection, improve stability, and maintain network synchronism [2]. The use of single-phase auto-reclosure has advantages such as providing the network stability by keeping two healthy phases connected to the system during SLG faults. In this situation, the synchronization conditions at the two ends of the TL are satisfied through two healthy phases and the synchronism of voltages and currents continues for a longer period. Today, single-phase auto-reclosures are widely used all over the world in high voltage TLs, because uninterrupted providing of the electricity is the first and foremost goal of power system operators. Furthermore, single-phase reclosures are categorized into two types of adaptive and nonadaptive reclosures [3]. Nonadaptive reclosure works according to specified times, i.e. it reconnects the faulted phase after one or multiple specified time delay periods regardless of the fault type. Nonadaptive reclosures are not capable of diagnosing the fault type and estimating the secondary arc extinguishing time when a transient fault occurs. In other words, when a transient SLG occurs, a severe

*Correspondence: Mohsen.Jannati@Shahreza.ac.ir

short-circuit current passes through the primary arc until the fault continues; however, the arc persistence is not substantial. Although the circuit breakers (CBs) on the sides of a TL disconnect the faulted phase from the power grid, two healthy phases continue working in the grid, and thus the capacitive coupling between the healthy and faulted phases produces an extremely high voltage in the faulted phase, thereby continuing the current and the secondary arc. Successful reclosing is not possible until the secondary arc is completely extinguished and, if unsuccessful, can lead to irreparable damage to the power system and in some cases may convert the transient fault to a permanent fault. Therefore, the use of nonadaptive reclosures may lead to unsuccessful reclosing operations and new problems. However, it is possible to improve the performance by use of adaptive reclosures equipped with microprocessor technology and computer systems. In other words, adaptive reclosures are able to recognize permanent faults from transient ones and block the reclosing function on permanent faults. Moreover, adaptive reclosures determine the minimum required time for a successful reclosing and thus prevent the loss of stability and synchronism in the TL, which consequently enhances the useful life of the reclosures located at the TL terminals [1].

Different methods have been presented for identifying transient faults from permanent faults in the literature. These methods are actually algorithms used for making single phase auto-reclosures more adaptive. In [4] a numerical algorithm based on total harmonic distortion (THD) factor was utilized for adaptive determination of dead time and preventing the single phase auto-reclosure during a permanent fault occurrence in heavy-loaded TLs. This algorithm is based on the input data processing at the TL terminal. In the algorithm proposed in [5], as the measured voltage waveform at the beginning or end of the TL is not suitable for using in neural networks, harmonic components of the voltage waveform are extracted and given to the artificial neural network (ANN), which makes decisions about the type of the faults. The specifications of the utilized ANN are given in [6]. Because wavelet transform can extract harmonic components along with the occurrence time, its coefficients are used as the ANN input in [7]. The ANN is pretrained so that it is capable of identifying transient faults from permanent faults accurately.

In order to detect secondary arc extinguishing time, the zero sequence power principle is employed in [8]. In [9], a numerical algorithm in the frequency domain is used to prevent unsuccessful reclosing during the permanent fault occurrence. Amplitude of the arc voltage and fault location are calculated via fundamental and third harmonics of the voltage and current phasors of the terminal. A criterion called dual-window transient energy ratio is presented in [10]. A concept of generalized multiresolution morphological gradient (GMMG) with multiresolution morphological gradient (MMG) is employed to extract the high-frequency energy of the current. In the adaptive single phase auto-reclosure algorithm proposed in [11], the RMS of the faulty phase voltage is measured continuously, and then the differences between the values of two following moments are calculated. If the difference is more than a threshold value, the algorithm infers that the secondary arc is stopped and reclosing can be successful. Otherwise, the fault is permanent although two healthy phases should be tripped as well.

Another strategy for adaptive single phase auto-reclosure in TLs equipped with a shunt reactor is presented in [12]. This approach is based on the difference between the current calculated through the transient fault model and the real current measured in the faulty phase of the shunt reactor. This strategy only works for TLs equipped with shunt reactors. In [13], a signal analysis scheme based on the PRONY algorithm is used for achieving the specifications of the shunt reactor current. The type of the fault is determined according to the frequency and fluctuations of different signals. This approach needs four-legged shunt reactors as well. The algorithm proposed in [14] is based on wavelet packet energy entropy, in which time-frequency features of

the faulty voltage are detected for recognition of the secondary arc and the fault type. In this approach, the faulty phase voltage is decomposed by a three-layer wavelet packet and then eight signals are reconstructed at the third level. Afterwards, the energy entropy of each scale is calculated according to the constructed signals. The practical implementation of this approach is very challenging. In [15], the harmonic of the faulty phase voltage is analyzed using wavelet packet transform and an integrated auto-reclosuer scheme is presented, which uses an adaptive threshold level. An adaptive reclosing scheme is proposed in [16], which is based on the wavelet transform of neutral current and uses a battery energy storage system (BESS). The proposed index for reclosing is developed by using the Symlets 5 mother wavelet at level 2. However, this method is applied to distribution networks. In [17], a detection method is presented which calculates the differential currents at the fault point. This scheme can be applied for three-phase reclosuers in TLs with shunt reactors. The authors in [18] analyze the features of faulty phase terminal voltage considering the neutral small reactance voltage as a base value. Then the ratio of faulty phase terminal voltage to neutral small reactance voltage for the measured and calculated values is achieved and the difference between them is used as a threshold for fault type recognition. In order to detect transient and permanent faults in [19], a low-pass filter and the cascaded delayed signal cancellation technique are applied to the voltage of the faulted phase. Transient faults are identified from permanent faults by using the average distortion rate and a threshold. This method is only applicable to TLs equipped with FLRs. The use of a threshold is another drawback of this scheme. The authors in [20] propose a three-phase adaptive reclosing scheme for TLs with FLRs by using the difference between the number of oscillating frequencies of faulted phase currents of FLRs before the fault extinction and after that. This method is applicable to TLs equipped with a FLR as well and also it can be used for three phase reclosure, which is rarely needed today. In [21], harmonics amplitudes are used as the criterion for the detection of secondary arc extinction, which is calculated after the TT transform. Although the used threshold level is adaptive, this scheme still needs a threshold. The authors in [22] present an auto-reclosure scheme for the synchronous generator type of distributed generation (DG) units to reduce DG oscillations after successful reclosing. The strength of this method is analyzing the conditions in the presence of DGs, but it is designed for distribution networks. Nevertheless, checking the unbalanced conditions mentioned in [23] is very useful. Also, in [24] and [25], the construction of a real-time single-phase auto-reclosure is carried out, although it is not investigated for double-circuit TLs.

On the other hand, capacitive coupling between healthy and faulted phases is the most effective factor in the current intensity and secondary arc duration. In addition, double-circuit TLs influence the coupling intensity considerably. In these TLs, the faulted phase has electrical and electromagnetical couplings with two other healthy phases of the same circuit and with the phases of the other circuit as well. As a result, the secondary arc current intensity and thus the induced voltage and the secondary arc extinguishing time increase. Therefore, many of the mentioned methods do not operate properly in double-circuit TLs because of the changes in voltage and current waveforms. Single-phase adaptive reclosure on double circuit TLs has been investigated in some studies; however, none of them considered all the situations in TLs. For example, in [26] only TLs equipped with FLRs are studied and situations such as use of high speed grounding switches (HSGS) for auxiliary equipment, different levels of TL voltage, different loadings, and noisy situations are not considered. In this paper, an accurate solution for detecting the fault type and estimating the secondary arc extinguishing time is proposed. These two operations are based on a new index using the harmonics of healthy TL current. In addition to its high accuracy and speed, the proposed method does not require any threshold level, neither for fault type detection nor for determining the extinguishing moment of the secondary arc (the

moment of issuing the successful reclosing command), and thus it is suitable for any type of double-circuit TL. The rest of the paper is organized as follows. Section 2 introduces the utilized arcing model. Section 3 describes the proposed method for detection of fault type and estimation of faulted phase reclosing time. The simulation results are presented in Section 4. Section 5 concludes.

2. Electrical power system model

2.1. Modeling of arcing fault

The arcing fault model introduced in [27] is utilized in this paper. The authors in [27] differentiated between arcs and categorized them into two types: 1) primary arcs occurring during the short circuit SLG fault and 2) secondary arcs resulting from capacitive coupling between healthy and faulty phases. Unlike the other models, this model has very close proximity to the practical results and is suitable for high voltage TLs. The arcing model used in this method is based on the energy balance of the arc column. The arc in the air can be described by a differential equation of the conductivity coefficient [28, 29]:

$$\frac{\mathrm{d}g}{\mathrm{d}t} = \frac{1}{\tau}(G - g), \tag{1}$$

where τ, g, and G are arc time constant, arc instantaneous conductivity, and arc constant conductivity, respectively. The arc constant conductivity is calculated by the following equation:

$$G = \frac{|i_{arc}|}{u_{st}}, \tag{2}$$

$$u_{st} = ({u_0}' + {r_0}'|i_{arc}|).l_{arc}(t), \tag{3}$$

where i_{arc}, u_{st}, l_{arc}, ${u_0}'$, and ${r_0}'$ indicate instantaneous arc current, constant arc voltage, instantaneous arc length, arc voltage characteristic, and arc resistance characteristic in terms of the length, respectively. Equation (1) is the general equation of the electric arc appropriate for expressing the arc in a bipolar electric circuit. Parameters τ, ${u_0}'$, and ${r_0}'$ are attained by measuring [23]. These parameters change with the arc length considerably for the secondary arc. The relation between τ and l_{arc} is defined by the following equation:

$$\tau = \tau_0 \left(\frac{l_{arc}}{l_0}\right)^{\alpha}, \tag{4}$$

where τ_0 is the primary time constant, l_0 is the primary arc length, and α is the empirical coefficient with a negative value. Since changes in the secondary arc length depend on external factors such as the wind and the intrinsic thermal conductivity, it is hard to consider all the factors precisely. However, the above arcing model can be used for estimating the maximum arc time at worst or for understanding the interaction between the secondary arc and the electric circuit. The most important part of the secondary arc modeling is defining the conditions in which the secondary arc extinguishes. In [23] the extinguishing criterion is of the secondary arc dielectric conditions type. The criterion for the final arc extinguishing is considered as follows:

$$\frac{\mathrm{dr}}{\mathrm{dt}} > \frac{\mathrm{dr}_{\min}}{\mathrm{dt}}, \quad g_{cal} < g_{min}, \tag{5}$$

where $\frac{\mathrm{dr}}{\mathrm{dt}}$ and g represent instantaneous resistance derivative with respect to time and instantaneous arc conductivity, respectively. If the value of the derivative is more than a specified value and the calculated

instantaneous arc conductivity is smaller than a specified value, the secondary arc extinguishes [30]. It should be noted that in this paper only SLG faults are investigated and other fault types such as phase-to-phase faults are not studied.

2.2. Studied double-circuit TLs

The typical power system in this study contains a 400 kV–50 Hz three-phase sinusoidal source with power generation capacity of 500 MW. This sinusoidal source is connected to an infinite bus through a double-circuit high voltage TL of 252 km in length. The mentioned TL has a DC resistance of 0.07052 Ω/km and an external diameter of 2.8143 cm. Since the basis of this study is the TL behavior during short circuit occurrence in the power frequency domain, the considered model for the TL is a model depending on frequency. A diagram of the double-circuit power system simulated in EMTP-RV is shown in Figure 1.

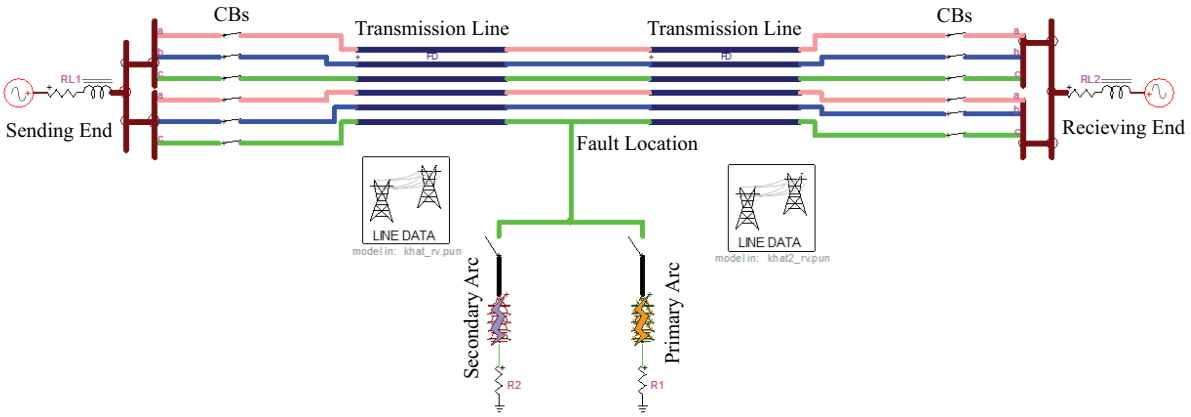

Figure 1. Studied double-circuit TL.

The parameters of the power system in Figure 1 are set as $X_{1S} = 191.87\Omega$, $X_{0S} = 46.75\Omega$ for the source at the sending end and $X_{1R} = 146.59\Omega$, $X_{0R} = 45.23\Omega$ for the source at the receiving end where X_{1S}, X_{0S}, X_{1R}, and X_{0R} are positive and zero sequence impedances at the sending end and the receiving end, respectively. The parameters of the TLs in Figure 1 are set as $R_1 = 0.02095\Omega/km$, $R_0 = 0.1495\Omega/km$, $X_1 = 0.28015\Omega/km$, $X_0 = 0.9412\Omega/km$, $C_1 = 0.01394\mu\,F/km$, $C_0 = 0.00901\mu\,F/km$, $C_m = 0.00138\mu\,F/km$, and $M_m = 0.0689H/km$ where R_1, R_0 are positive and zero sequence reactance per length of the line; X_1, X_0 indicate positive and zero sequence reactance per length of the line; C_1, C_0 are positive and zero sequence capacitance per length of the line; C_m is coupling capacitance of the lines; and M_m denotes the mutual inductance of the lines.

In order to survey and analyze the presented fault model in Section 2.1, a bus is appended to an arbitrary location on the TL and then the selected arcing model (including primary and secondary arcing models) is placed at that location. Primary and secondary arc models include a measuring switch in series with the resistance acquired by solving the equation introduced in Section 2.1. Figure 2a and Figure 2b show voltage waveforms at the beginning of the TL and fault location current waveform (in the middle of the TL), respectively, during permanent SLG fault occurrence. Although the fault location voltage waveform is available in simulation results, it is not available in practice. Also, only the current of the current transformer is practically available at the beginning or end of the TL, although it becomes zero after the operation of CBs.

Figure 3 and Figure 4 show voltage waveforms at the beginning of the TL and fault location current waveform, respectively, in the middle of the TL during the transient SLG fault occurrence. According to the description in Section 1, the current of the transient fault contains both the primary arc current and the secondary arc current shown in Figure 4a and Figure 4b, respectively. It is also evident that the secondary arc current is substantially lower than the primary arc current.

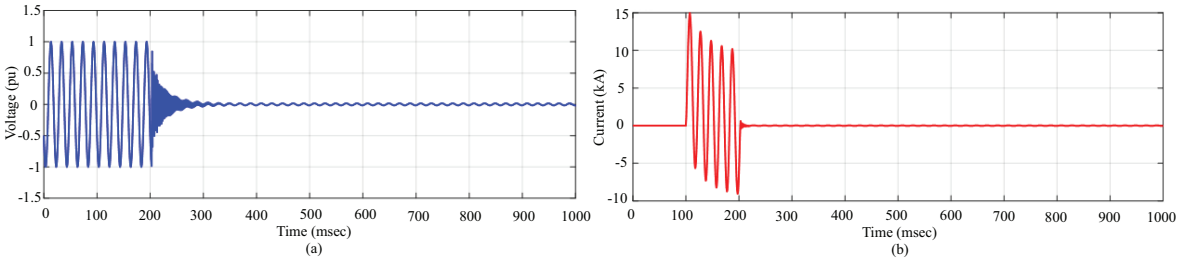

Figure 2. a) Voltage waveform at the beginning of TL and b) fault location current waveform when a permanent SLG fault occurs.

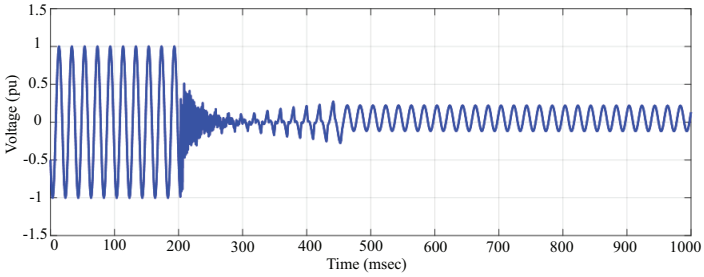

Figure 3. Voltage waveform at the beginning of TL when transient SLG fault occurs.

3. Proposed scheme for identifying fault type and faulty phase reclosing time

3.1. Analyzing voltage and current waveforms of the healthy circuit during the occurrence of transient and permanent faults

It is necessary to analyze voltage and current waveforms of the healthy circuit during the fault occurrence in order to detect fault type (transient or permanent) in double-circuit TLs through the harmonic analysis of the healthy circuit phases. In the following, voltage and current waveforms of the healthy circuit are extracted and the possibility of harmonic analysis through the waveforms is reviewed. The voltage waveforms at the beginning and fault location of the healthy circuit during the transient fault occurrence are shown in Figure 5a and Figure 5b, respectively. Figure 5c shows the current waveform of a healthy circuit during the transient fault occurrence. It is clear that the voltage at the beginning of the TL does not show any changes and thus it is not suitable for analysis. The waveform of the healthy phase at the fault location has good variations; however, it cannot be a suitable criterion because it is unavailable in practice. The current waveform of the healthy phase has suitable changes so it can be used as a criterion. The voltage waveforms at the beginning and fault location of the adjacent circuit during the permanent fault occurrence are shown in Figure 5d and Figure 5e, respectively. Figure 5f shows the current waveform of the adjacent circuit during the permanent fault occurrence. In this case, like the transient fault, the voltage waveforms of the fault location are not available

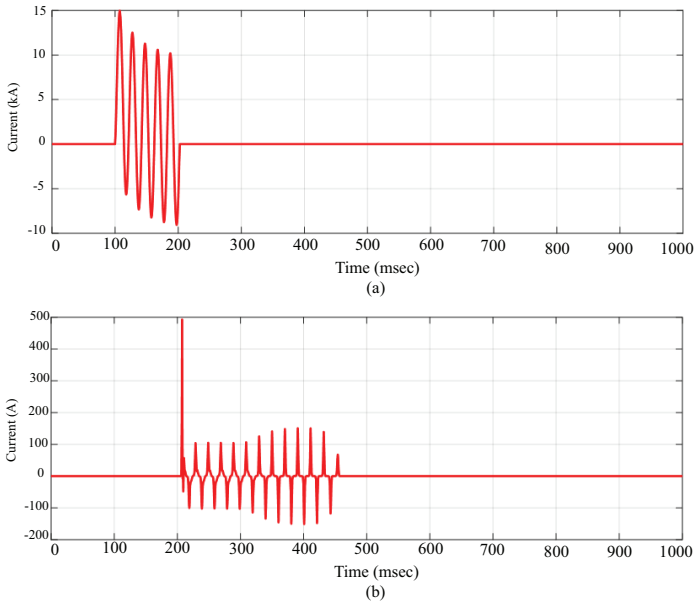

Figure 4. Fault location current waveforms when transient SLG fault occurs: a) primary arc, b) secondary arc.

practically. On the other hand, voltage waveforms at the beginning of healthy circuit phases are sampled from a location behind the circuit breaker and thus there would be no change in the voltage magnitude of achieved samples and the required harmonics could not be acquired consequently. This is the reason for using current harmonic analysis of the healthy circuit phases for diagnosing permanent and transient faults from each other as well as determining the secondary arc extinguishing time, which is the time of successful adaptive reclosing.

3.2. Identifying fault type and faulty phase reclosing time

Current of the adjacent circuit phases carrying the load current is used for fault type detection in this study. When a short-circuit SLG fault occurs, circuit breakers of both ends trip the relevant phase after a time delay related to the function of the protective equipment. The secondary arc has a nonlinear nature and thus the current of the secondary arc is nonsinusoidal (Figure 4b). This current makes a field inducing nonsinusoidal voltage in two healthy phases of the first circuit and in healthy phases of the other circuit. Consequently, harmonic components appear in the healthy phase currents of both circuits. Existence of these components indicates that the fault is transient. If the fault is transient, then the ending time of the secondary arc is determined. It is feasible to apply this method to the current waveform because of the acceptable bandwidth of the current transformers. In other words, this method does not encounter hardware limitations. Signals sampled from the current of the healthy circuit's three phases are added together and residual current (I_r) is acquired. The value of residual current is zero before fault occurrence when the system is working in a balanced symmetrical mode. As a fault occurs, the system exits from normal operation and thus the algebraic sum of the asymmetric three phases' currents is not zero anymore. This current is different from zero-sequence current. Figure 6a and Figure 6b illustrate residual current waveforms in healthy circuits when permanent and transient short-circuit SLG faults occur, respectively. Although the waveforms in Figure 7a and Figure 7b may look alike, they have differences observable when their harmonics are analyzed separately. In order to obtain the

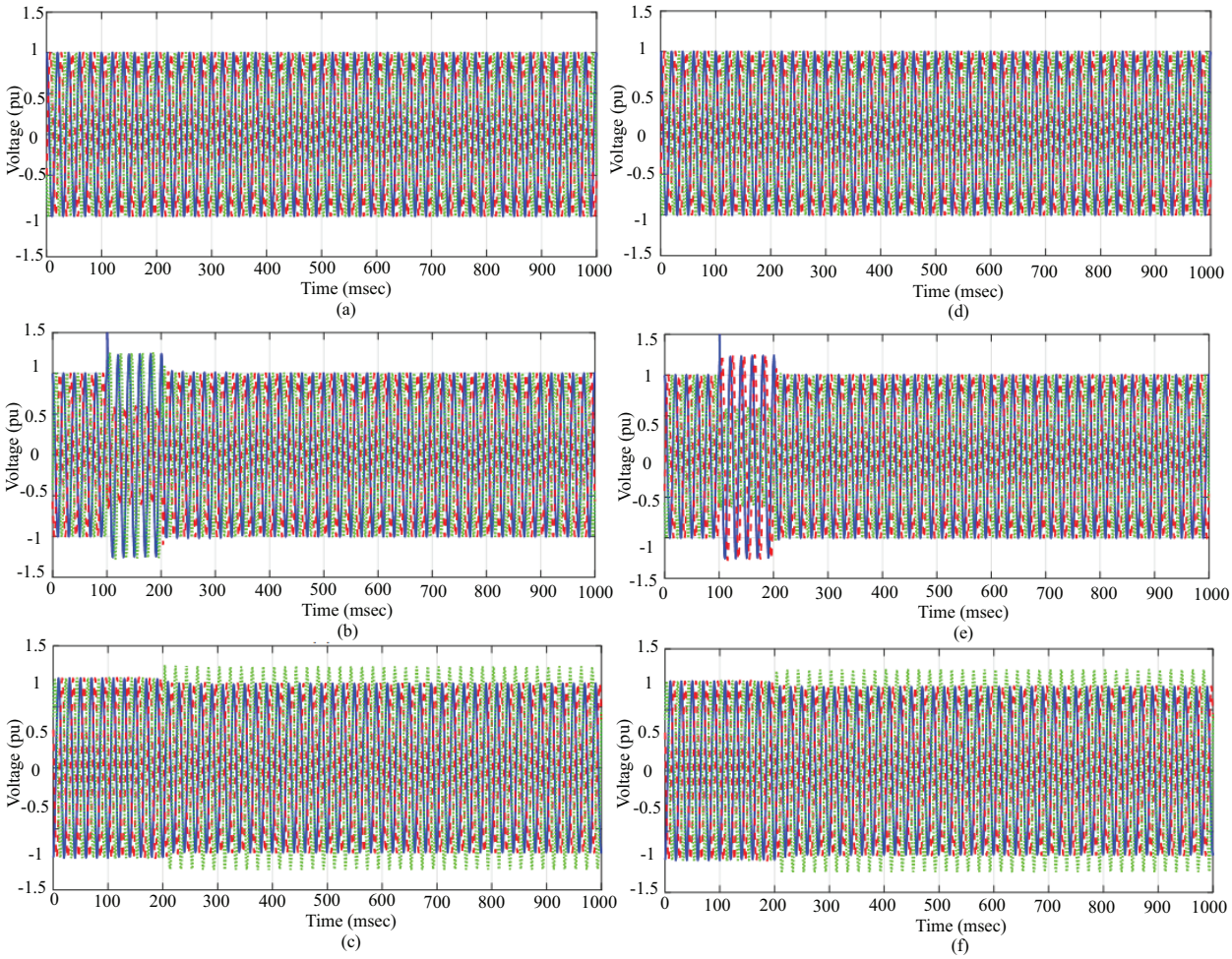

Figure 5. a) Voltage waveform at the beginning of the healthy circuit. b) Voltage waveform at the fault location in the healthy circuit. c) Current waveform of the healthy circuit when a transient SLG fault occurs. d) Voltage waveform at the beginning of the adjacent circuit. e) Voltage waveform at the fault location in the adjacent circuit. f) Current waveform in the adjacent circuit when a permanent SLG fault occurs.

required index for detecting fault type, the first to ninth harmonics of residual currents are extracted. For this purpose, the kth harmonic of the input signal instantaneous value is converted to a phasor in the reference framework around the main frequency. The expression (x, y) includes x, y coordinates of calculated harmonics in the reference framework. x, y coordinates of the phasor are calculated on a floating time interval with a period of $\frac{1}{f}$ as follows:

$$x = \frac{2}{cycle} \int_{t-cycle}^{t} in(t).\cos(k2\Pi ft)\mathrm{d}t \quad , \quad y = \frac{2}{cycle} \int_{t-cycle}^{t} -in(t).\sin(k2\Pi ft)\mathrm{d}t, \tag{6}$$

$$magnitude = \sqrt[2]{x^2 + y^2}. \tag{7}$$

Figure 7a and Figure 7b show the odd harmonics of residual current when permanent and transient SLG fault occurs, respectively. The different behavior of the harmonics in the transient and permanent faults

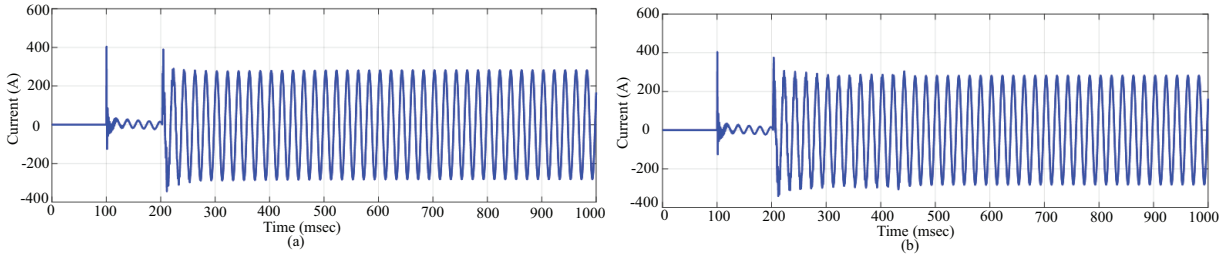

Figure 6. Residual current waveform when a) permanent and b) transient short-circuit SLG fault occurs.

after the fault occurrence can be observed at the time 230 ms in Figure 7a and Figure 7b. Therefore, it is necessary to extract a suitable harmonic index based on these waveforms to distinguish between permanent and transient states. Various indexes based on the harmonics resulting from permanent and transient faults were tested. However, some of these indexes were removed for some reasons such as lack of required accuracy in fault type detection or in detecting secondary arc extinguishing time. Finally, the appropriate harmonic index was extracted from the residual current harmonics. Equation 8 shows the proposed index having the required accuracy in detecting fault type and secondary arc extinguishing time:

$$HI_{Index} = \frac{|h_3|}{\sqrt[2]{\sum_{n=1}^{5} |h_{2n-1}|^2}}, \tag{8}$$

where HI_{Index} is the harmonic index, h_3 is the third harmonic of residual current, and h_{2n-1} indicates odd harmonics of residual current. As the third harmonic of residual current is in the numerator, it is the dominant harmonic in the above equation. In order to increase the value of the harmonic index for more accurate fault type detection, the odd harmonics in the denominator are squared. Harmonic index for a transient fault is shown in Figure 8a. As shown in Figure 8, a short-circuit SLG fault has occurred at t = 100 ms. Circuit breakers receive a trip command for the faulted phase after about 100 ms as a result of protective equipment action. At 30–50 ms after receiving the trip command, breakers have disconnected both sides of the faulted phase completely. At this moment, the primary arc is completely extinguished and the secondary arc appears. After passing a few cycles from the secondary arc's appearance moment, the arc length increases. At the moment of fault current zero crossing, the insulation resistance of the arc path is retrieved and the current remains at the value of zero. As the voltage to earth of the fault location increments, the applied voltage may lead to the insulation failure of the arc path and thus the fault current is established again. In each cycle this process repeats until the condition of the final extinguishing is achieved. Since the priority for disconnecting the faulted phase is with the distance relay, it is not necessary to check the proposed index until the distance relay issues the tripping command. With this aim, the behavior of the proposed index is evaluated as the CBs are disconnected after receiving the command from the distance relay and passing a very short time in the range of several power cycles. Figure 8b illustrates the behavior of the index when several cycles are passed after tripping the faulted phase.

The dashed curve in Figure 8b shows the harmonic index for a permanent fault from the moment of complete tripping. Disturbing distortions have been removed through the moving average technique. The solid curve in Figure 8b shows the improved harmonic index. As illustrated in Figure 9a, in the case of a permanent

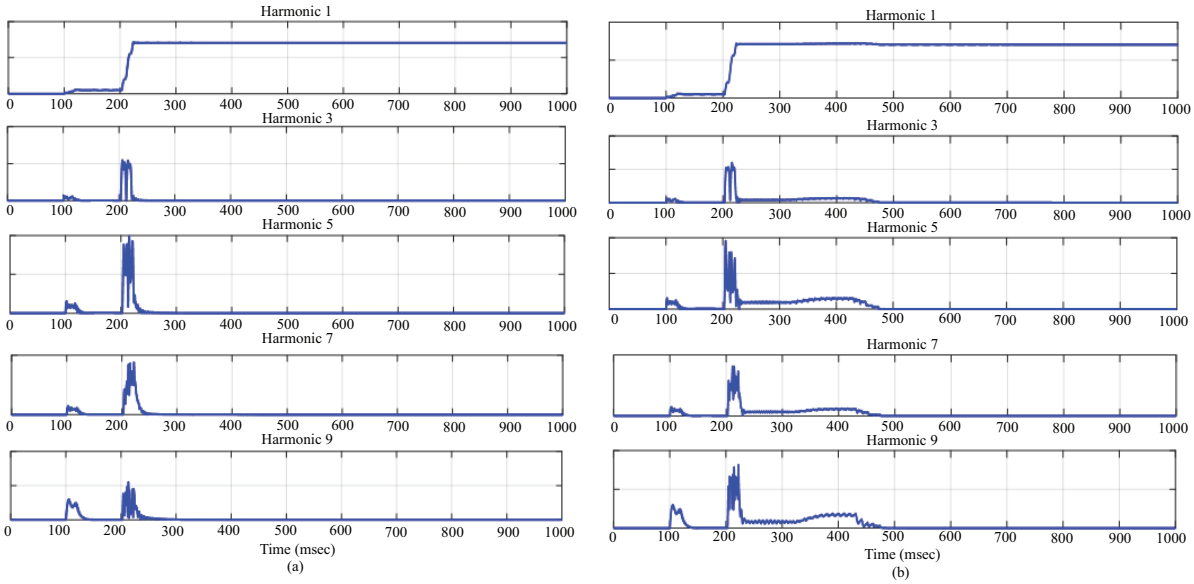

Figure 7. Waveforms of residual current odd harmonics when a) permanent and b) transient SLG fault occurs (harmonics one to nine).

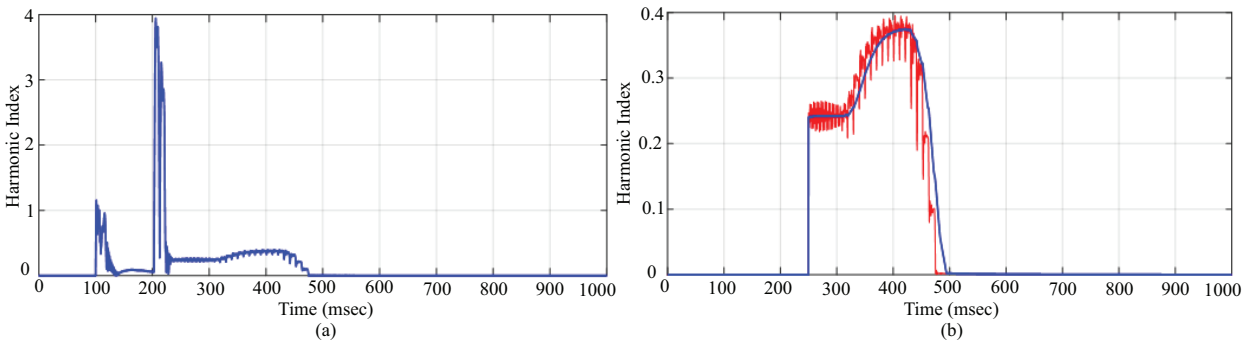

Figure 8. a) Harmonic index when a transient SLG fault occurs. b) Harmonic index after CB tripping and applying the moving average technique.

fault, the primary arc is extinguished after the CB trips. The secondary arc is not established because of the permanent fault nature. This is clear in the figure. Therefore, the proposed harmonic index is capable of detecting permanent faults from transient faults. According to the description in the section on transient fault, since the priority for tripping the faulted phase is with the distance relay, the proposed index is not evaluated until the distance relay issues the tripping command. Figure 9b illustrates the behavior of the proposed index when several cycles are passed after tripping the faulted phase. The dashed curve in Figure 9b shows the harmonic index for a permanent fault from the moment of complete tripping. Disturbing distortions have been removed through the moving average technique. The solid curve in Figure 10 shows the improved harmonic index.

In order to better illustrate the different behaviors of the proposed index in transient and permanent fault cases, the harmonic index is shown in Figure 10. As illustrated in Figure 10, in the case of permanent faults, the harmonic index trend is descending after the tripping, i.e. $HI(t+\Delta t) < HI(t)$. However, in the case of a

transient fault, the harmonic index is ascending, i.e. $HI(t+\Delta t) > HI(t)$. In this case, as the secondary arc extinguishes, the value of harmonic index reaches zero, i.e. $HI(t) = 0$. In other words, after opening the CBs, if $HI(t+\Delta t) < HI(t)$ the SLG fault is permanent and the tripping command is sent for two healthy phases as well. However, if $HI(t+\Delta t) >= HI(t)$, the fault is declared as transient and the algorithm tries to detect the extinguishing moment of the secondary arc to issue a successful reclosing. If $HI(t+\Delta t) - HI(t) = 0$, it means that the time of successful reclosing is reached and the algorithm will issue a reclosing command to the faulted phase.

The proposed algorithm for fault type detection along with determining secondary arc extinguishing time (for transient faults) is given in Figure 11.

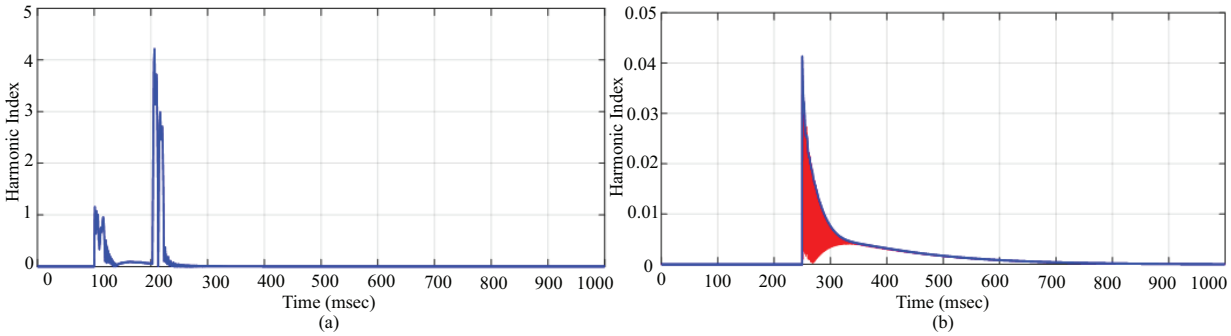

Figure 9. a) Harmonic index when a permanent SLG fault occurs. b) Harmonic index after CB tripping and applying the moving average technique.

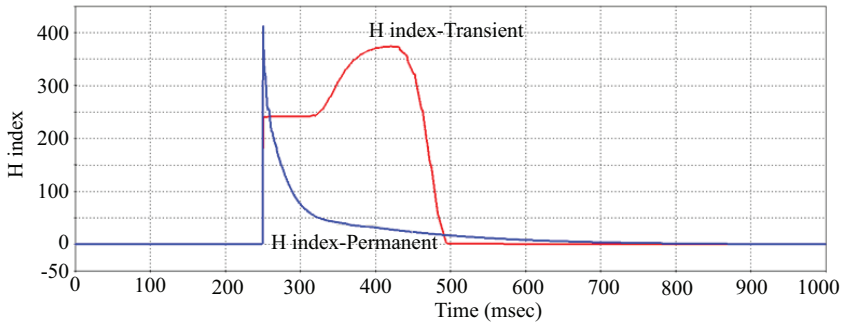

Figure 10. Harmonic index behavior: a comparison between transient and permanent faults.

4. Simulation results

In addition to different fault conditions considered in this section for the performance evaluation of the proposed scheme, simulations have been implemented and assessed in different situations such as transposed or nontransposed TL of the studied network in Section 2.2, equipped with or not equipped with auxiliary equipment like HSGSs or FLRs for a faster extinguishing of the secondary arc, different locations for the SLG fault in different phases of the double circuit TL, different levels of voltage, etc. The simulation results are presented in Table 1. The values of precision in Table 1 are the lowest among the values achieved for the situations in each row. Also, each situation is simulated for all the fault locations in phase A, B, and C in 10 km intervals of the TL. The

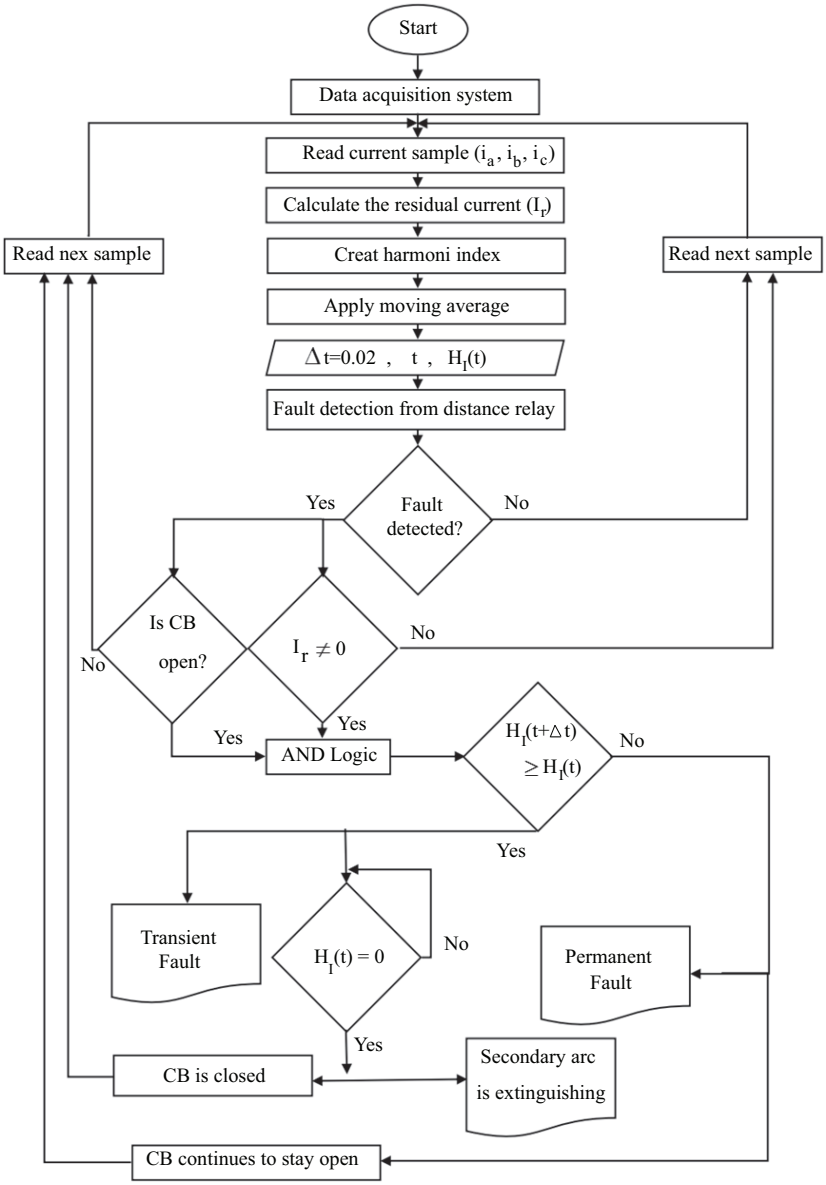

Figure 11. Flowchart of the proposed method.

simulation results presented in Table 1 show that the proposed algorithm works correctly in at least 97.14% of situations, and it is able to detect the fault type and extinguishing moment of the secondary arc precisely. Then the proposed scheme is compared with other schemes considering 280 different scenarios. The criterion used in [4] is the faulted phase voltage THD while the method in [15] uses wavelet packet transform and an adaptive threshold level based on the harmonic of the faulted phase voltage. The proposed criterion in [19] is based on a low-pass filter and the cascaded delayed signal cancellation technique, which is applied to the faulted phase voltage. The approach proposed in [25] is a method based on the voltage harmonic content measurement. The method in [26] uses the difference between the calculated and the measured voltage of the faulted phase across

the FLR although it is designed only for double circuit TLs equipped with FLRs. Table 2 presents the results of the evaluated approaches. As seen, the suggested algorithm in this study has the highest precision compared with the others.

Table 1. Simulation results.

Situation	Transposed	Auxiliary equipment	Number of events	Correct diagnosis	Precision
Fault located in phase A, B, and C in 10 km intervals	×	×	200	199/200	99.50%
Fault located in phase A, B, and C in 10 km intervals	✓	×	200	200/200	100.00%
Fault located in phase A, B, and C in 10 km intervals	✓	HSGS	150	146/150	97.33%
Fault located in phase A, B, and C in 10 km intervals	✓	FLR	150	148/150	98.66%
Voltage levels of TL set to 230, 400, and 500 kV	✓	×	150	148/150	98.66%
Power factor of loads set to the interval [0.8, 0.95]	✓	×	150	150/150	100%
Fault resistance set to 50, 100, 250, 300, and 500Ω	✓	×	150	150/150	100%
Noisy situations with SNR=20 and SNR=40	✓	×	80	78/80	97.50%
Harmonic load added at receiving end	✓	×	50	68/70	97.14%

Table 2. Evaluation results.

Scheme	Number of events	Transposed equipment	Auxiliary scheme	Adaptive	Precision
Method proposed in [4]	280	×	FLR	✓	87.11%
Method proposed in [15]	280	✓	FLR	✓	91.07%
Method proposed in [19]	280	✓	FLR	✓	91.78%
Method proposed in [25]	280	✓	FLR	✓	88.21%
Method proposed in [26]	280	✓	FLR	✓	92.85%
Proposed algorithm	280	✓	FLR	✓	97.14%

5. Conclusion

In this paper, a new approach is proposed for recognizing permanent faults from transient faults. In addition, the extinction time of the secondary arc (the moment of successful reclosing) is determined for utilizing in adaptive single phase auto-reclosures of double-circuit TLs. The proposed approach is based on the current harmonic analysis of healthy adjacent TL. The harmonics of the current waveform at the beginning of the healthy TL are extracted and then an index is presented for fault type recognition. Utilizing this method for

double-circuit TLs leads to a fast adaptive reclosing in the case of transient fault occurrences. Therefore, it prevents instability and nonsynchronism in two sides of the TL. Simulations performed in EMTP-RV verify the capability of the proposed approach to recognize the fault type and the secondary arc extinction time accurately in addition to its simple practical implementation.

References

[1] Jannati M, Vahidi B, Hosseinian SH, Ahadi SM. A novel approach to adaptive single phase auto-reclosing scheme for EHV transmission lines. International Journal of Electrical Power & Energy Systems 2011; 33 (3): 639-646. doi: 10.1016/j.ijepes.2010.12.023

[2] Wang X, Yang J, Liu P, Liu W, Yan J et al. Online calculation for the optimal reclosing time of transmission lines. Electric Power Components and Systems 2016; 44 (17): 1-13. doi: 10.1080/15325008.2016.1199071

[3] Jannati M, Jazebi S, Vahidi B, Hosseinian SH. A novel algorithm for fault type fast diagnosis in overhead transmission lines using hidden markov models. Journal of Electrical Engineering & Technology 2011; 6 (6): 742-749. doi: 10.5370/JEET.2011.6.6.742

[4] Radojevic ZM, Shin JR. New digital algorithm for adaptive reclosing based on the calculation of the faulted phase voltage total harmonic distortion factor. IEEE Transactions on Power Delivery 2007; 22 (1): 37-41. doi: 10.1109/TPWRD.2006.886781

[5] Aggarval RK, Johns AT, Dunn RW, Fitton DS. Neural network based adaptive single-pole autoreclosure technique for EHV transmission system. IEE Proceedings - Generation, Transmission and Distribution 1994; 141 (2): 155-160. doi: 10.1049/ip-gtd:19949864

[6] Yu IK, Song YH. Wavelet transform and neural network approach to developing adaptive single-pole auto-reclosing scheme for EHV transmission system. IEEE Power Engineering Review 1998; 18 (11): 62-64. doi: 10.1109/39.726911

[7] Radojevic ZM, Shin JR. New one terminal digital algorithm for adaptive reclosing and fault distance calculation on transmission lines. IEEE Transactions on Power Delivery 2006; 21 (3): 1231-1237. doi: 10.1109/TPWRD.2005.860285

[8] Elkalashy NI, Darwish HA, Taalab AI, Izzularab MA. An adaptive single pole autoreclosure based on zero sequence power. Electric Power System Research 2007; 77 (5): 438-446. doi: 10.1016/j.epsr.2006.04.006

[9] Lin X, Weng H, Liu H, Lu W, Liu P et al. A novel adaptive single-phase reclosure scheme using dual-window transient energy ratio and mathematical morphology. IEEE Transactions on Power Delivery 2006; 21 (4): 1871-1877. doi: 10.1109/TPWRD.2006.881427

[10] Yaozhong G, Fanghai S, Yuan X. Prediction method for preventing single-phase reclosing on permanent fault. IEEE Transactions on Power Delivery 1989; 4 (1): 114-121. doi: 10.1109/61.19197

[11] Quoc TT, Hadj-Said N, Sabonnadiere JC, Feuillet R. Reducing dead time for single-phase auto-reclosing on a series-capacitor compensated transmission line. IEEE Transactions on Power Delivery 2000; 15 (1): 51-56. doi: 10.1109/61.847228

[12] Suonan JL, Sun DD, Fu W, Wang XB, Liu WT et al. Identification of permanent faults for single-phase autoreclosure on transmission lines with shunt reactors. In: Proceedings of CSEE; Oahu, HI, USA; 2006. pp. 75–81. doi: 10.1109/tpwrd.2009.2014475

[13] Chothani NG, Bhalja BR, Desai AK. A new algorithm for coordination of relay and auto-reclosure in 220 kV transmission system. In: India Conference (INDICON); Mumbai, India; 2013. pp. 1-6. doi: 10.1109/INDCON.2013.6726062

[14] Haitao Z, Chen Ping, Li-Ping W. Adaptive reclosure technology for high-voltage overhead lines combined with underground power cables based on travelling wave principle. In: Proceedings of the 2012 International Conference on Communication, Electronics and Automation Engineering; Xi'an, China; 2012. pp. 143–150

[15] Adly AR, Sehiemy RA, Abdelaziz AY. An optimal/adaptive reclosing technique for transient stability enhancement under single pole tripping. Electric Power Systems Research 2017; 151: 348-358. doi: 10.1016/j.epsr.2017.06.005

[16] Seo H, Rhee S. Novel adaptive reclosing scheme using wavelet transform in distribution system with battery energy storage system. International Journal of Electrical Power & Energy Systems 2018; 79: 186-200. doi: 10.1016/j.ijepes.2017.11.009

[17] Shao W, Liu Y, Zhang W. Nonfault detection for three-phase reclosure in reactor-compensated transmission lines based on fault location. In: 5th International Conference on Electric Utility Deregulation and Restructuring and Power Technologies (DRPT); Changsha, China; 2015. pp. 1-4. doi: 10.1109/DRPT.2015.7432370

[18] Jiaxing N, Baina H, Zhenzhen W, Jie K. Algorithm for adaptive single-phase reclosure on shunt-reactor compensated extra high voltage transmission lines considering beat frequency oscillation. IET Generation, Transmission & Distribution 2018; 12 (13): 3193-3200. doi: 10.1049/iet-gtd.2017.1175

[19] Xie X, Huang C. A novel adaptive auto-reclosing scheme for transmission lines with shunt reactors. Electric Power Systems Research 2019; 171: 47-53. doi: 10.1016/J.EPSR.2019.01.028

[20] Luo X, Huang Ch, Jiang Y, Guo S. An adaptive three-phase reclosure scheme for shunt reactor-compensated transmission lines based on the change of current spectrum. Electric Power Systems Research 2018; 158: 184–194. doi: 10.1016/J.EPSR.2018.01.011

[21] Nikoofekr I, Sadeh J. Determining secondary arc extinction time for single-pole auto-reclosing based on harmonic signatures. Electric Power Systems Research 2018; 163: 211-225. doi: 10.1016/j.epsr.2018.06.013

[22] Abedini M, Sanaye-Pasand M, Davarpanah M, Lesani H, Shahidehpour M. Predictive auto-reclosure approach to enhance transient stability of grid-connected DGs. IET Generation, Transmission & Distribution 2019; 13 (14): 3011–3019. doi: 10.1049/iet-gtd.2018.6455

[23] Hernández JC, Ruiz-Rodriguez FR, Jurado F. Technical impact of photovoltaic-distributed generation on radial distribution systems: stochastic simulations for a feeder in Spain. International Journal of Electrical Power & Energy Systems 2013; 50: 25-32. doi: 10.1016/j.ijepes.2013.02.010

[24] Monadi M, Hooshyar H, Vanfretti L. Design and real-time implementation of a PMU-based adaptive autoreclosing scheme for distribution networks. International Journal of Electrical Power & Energy Systems 2019; 105: 37-45. doi: 10.1016/J.IJEPES.2018.07.064

[25] Dias O, Tavares MC, Magrin F. Hardware implementation and performance evaluation of the fast adaptive single-phase auto reclosing algorithm. Electric Power Systems Research 2019; 168: 169-183. doi: 10.1016/j.epsr.2018.11.019

[26] Shang L. Fault nature identification for single-phase adaptive reclosure on double circuit EHV transmission lines with shunt reactors. In: International Conference on High Voltage Engineering and Application; New Orleans, LA, USA; 2010. pp. 1-4. doi: 10.1109/ichve.2010.5640714

[27] Kizilcay M, Ban G, Prikler L, Handl P. Interaction of the secondary arc with the transmission system during single-phase autoreclosure. In: IEEE Bologna Power Tech Conference Proceedings; Bologna, Italy; 2003. pp. 1-20. doi: 10.1109/PTC.2003.1304294

[28] Prikler L, Kizilcay M, Ban G, Handle P. Improved secondary arc models based on identification of arc parameters from staged fault test records. In: 14PSCC; Seville, Spain; 2002. pp. 1-7

[29] Kizilcay M, Koch KH. Numerical fault arc simulation based on power m tests. European Transactions on Electrical Power 1994; 4 (3): 177-186. doi: 10.1002/etep.4450040302

[30] Johns AT, Aggarwal RK, Song YH. Improved techniques for modeling fault arcs on faulted EHV transmission systems. IEE Proceedings - Generation, Transmission and Distribution 1994; 141 (2): 148-154. doi: 10.1049/ip-gtd:19949869